JOURNAL OF MATERIALS SCIENCE **40** (2005) 871–874

Faceting of the Σ3 coincidence tilt boundary in Nb

B. B. STRAUMAL*, V. N. SEMENOV, A. S. KHRUZHCHEVA
Institute of Solid State Physics, Russian Academy of Sciences, 142432 Chernogolovka, Moscow District, Russia
E-mail: (pop3) straumal@issp.ac.ru; (internet) straumal@mf.mpg.de

TADAO WATANABE
Laboratory of Materials Design and Interface Engineering, Department of Machine Intelligence and Systems Engineering, Graduate School of Engineering, Tohoku University, Sendai 980-8579, Japan

Due to their unusual properties, the grain boundaries (GBs) with the lowest possible inverse density of coincidence sites $\Sigma=3$ play a special role in the GB engineering. The as-grown shape of the cylindric tilt grain boundary (GB) in Nb bicrystal grown by the floating zone method has been studied with the electron back-scattering diffraction method. Both grains form the superlattice called coincidence site lattice (CSL) with the lowest possible inverse density of coincidence sites $\Sigma=3$. Four different CSL facets $(100)_{\Sigma3CSL}$, $\{110\}_{\Sigma3CSL}$, $\{120\}_{\Sigma3CSL}$ and $\{210\}_{\Sigma3CSL}$ were observed simultaneously. Flat facets $(100)_{\Sigma3CSL}$, $\{110\}_{\Sigma3CSL}$, $\{120\}_{\Sigma3CSL}$ and $\{210\}_{\Sigma3CSL}$ form smooth edges (no slope discontinuity) with rounded rough GB portions. Rough surface curves away from the plane of the $(-1, 2, 0)_{\Sigma3CSL}$ facet at the edge with $(-1, 1, 0)_{\Sigma3CSL}$ facet as x^{β} with $\beta = 1.61 \pm 0.09$. At the edge between $(210)_{\Sigma3CSL}$ and $(-1, 2, 0)_{\Sigma3CSL}$ facets $\beta = 1.46 \pm 0.09$. Both values reveal the GB roughening belonging to the Pokrovsky-Talapov universality class. It has been shown for Pb surfaces [K. Arenhold, S. Surnev, P. Coenen, H.P. Bonzel and P. Wynblatt, *Surf. Sci.* **417** (1998) L1160] that the β value depend on the details of the steps interaction at the vicinal surface. In our case the difference between measured β for two different facet edges can be due to the similar details of GB steps.

1. Introduction

The low-Σ grain boundaries (GBs), Σ being the inverse density of coincidence sites, and their faceting play a very important role in the GB engineering. Particularly, it has been observed that the fraction of faceted GBs decrease with increasing temperature in various materials like alumina [1], stainless steel [2], silver [3] and nickel-based superalloys [4]. The presence of GB faceting correlates in these materials with the phenomenon of abnormal grain growth. Above certain temperature the faceted GBs are absent and the abnormal grain growth does not appear [1–4]. The roughening phase transition can be the reason for the disappearance of faceted GBs [1–5]. The influence of the GB faceting is not occasional, since only so-called special GBs with misorientation angle θ close to a coincidence misorientation θ_{Σ} can facet. Special GBs exist in certain areas of θ and temperature. Particularly, the maximal temperature where GBs possess their special structure and properties decreases with increasing Σ [6]. It means that with decreasing temperature the number of special GBs increases, and the total angular interval for GBs able to facet increases as well. On the other hand, it has been observed that in certain materials the number of low-Σ GBs is surprisingly high [7–11]. The number of low-Σ GBs exceeds the theoretical value for a random polycrystal, derived by Mackenzie [12]. Particularly the frequency of Σ3 GBs can reach almost 30% in Ni in comparison with Mackenzie value of 6 to 8% [7]. It has been demonstrated that the production method, mechanical or thermal treatment, as well as annealing in magnetic field can influence the occurrence frequency of low-Σ and particular that of Σ3 GBs [1, 7, 10, 13]. The increase of number of Σ3 and Σ9 GBs is accompanied by the marked improvement of properties [14], particularly it decreases the GB corrosion [15]. In some cases the number of low-Σ GBs other than Σ3 in a polycrystal was almost negligible [16–18]. The high number of Σ3 GBs in polycrystals can be explained by the very broad angular interval of misorientations $\Delta\theta = |\theta - \theta_{\Sigma}|$ where Σ3 GBs possess their special structure and properties. The data on GB energy measurements in Al and NiO and on the structural investigations in Al, Pb and Au deliver the value of as high as 10 to 20° [19–25]. Therefore, the investigation of faceting of Σ3 GBs is so important for the GB engineering, especially for the control of fracture and corrosion properties of polycrystals and improvement

*Author to whom all correspondence should be addressed.

of their behavior by changing the spectrum of GB inclinations.

In spite of the technological importance of bcc metals having high melting temperature T_m only few facts are known about their GB faceting. The reason for that may be the high tendency to GB roughening in bcc metals. If it is true, the transition from faceted to rough GBs may be observed in bcc metals. Such transitions have been recently observed on free surfaces [26–30]. The formalism has been developed for the description of faceting-roughening phase transitions of second order using so-called critical indexes [26–30]. To the best of our knowledge, GB faceting-roughening has been never studied before using such approach. Due to their less pronounced GB faceting (in comparison with GBs in fcc metals) the bcc metals (including Nb chosen for the investigation in this work) could be the good candidates for investigation of GB faceting-roughening phenomena and measurements of respective critical indexes.

2. Experimental

For the investigation of GB shape, a cylindrical Nb bicrystal having diameter of 11 mm with two coaxial grains was grown by the floating zone technique [31, 32] from Nb of 99.95 wt% purity. To stabilize the temperature distribution in the liquid zone, a circular water-cooled copper electron gun was used. To prepare single crystalline seeds of different orientations, a single crystal was grown and cut to obtain cylindrical pieces of 15–20 mm length and 10–25 mm diameter. Two parallel surfaces of a seed were checked carefully by X-ray diffraction with an accuracy of about 1° and carefully polished in order to make very clean and mirror-like surfaces. The upper surface, normal to the growth axis of the seed holder, was prepared by cutting, grinding and polishing. Both ends of the initially cylindrical Nb ingots were cut normally to the growth axis and polished. Before growing, the lower holder with a seed on top of it, a cylindrical ingot and an upper holder were joined together by *in-situ* local electron-beam welding of the contacting surfaces. The seeding procedure consists of melting of a narrow liquid zone in the seed just under the seed/ingot interface. After an initial liquid zone is created, the electron gun is being moved up vertically together with the liquid zone until the whole specimen would become single crystalline. Thus, after such a procedure the single crystalline seed and zone-remelted specimen represent one elongated grain which has the same crystallographic orientation in all areas. A seed is then cut off from a grown single crystal by a spark erosion machine. The interior cylindrical grain 1 with diameter about 4.5 mm in the cylindrical coaxial Nb bicrystal is surrounded by the exterior ring grain 2 forming the $\Sigma3\langle110\rangle$tilt GB. The low growth rate of 1 mm/min ensures that the *as grown* GB shape nearly corresponds to the equilibrium one for (0.9–1.0) T_m. 2.0 mm thick platelets were cut from the grown bicrystal perpendicularly to the growth axis. GB is perpendicular to the both faces of the platelet. The platelets were ground with 4000 SiC paper, polished with 3 and 1 μm diamond paste and chemically polished in the hot (about 80°C) HF:$HNO_3$1:1 mixture. The electron back-scattering diffraction (EBSD) method has been used by us in order to determine the orientation of individual grains in the Nb bicrystal and the shape of the GB in the as-grown bicrystals. The EBSD method permits to observe the microstructure of the sample and to determine the orientation of the individual grains in the same experiment. The EBSD-patterns were measured with the aid of Hitachi S-4200 instrument. The spatial resolution of this instrument in the EBSD regime reaches 50 nm. In our measurements due to the large investigation field the 20 μm step between analysis point has been chosen. We have determined the orientation of the individual grains using the integrated software package for semi-automated fit procedure for indexing of the EBSD patterns.

3. Results and discussion

The section of $\Sigma3$ CSL perpendicular to the $\langle110\rangle$ axis is shown in the Fig. 1. The most closely packed CSL planes are shown together with respective planes for the lattices 1 and 2 forming CSL. For example the $(100)_{\Sigma3CSL}$ plane is also $(111)_1/(111)_2$. It has been demonstrated that $\Sigma3$ GB in Cu and Ag remains faceted up to the melting temperature T_m [33–35]. In other words, the roughening temperature T_R is higher than T_m for the $(100)_{\Sigma3CSL}$ facet and the non-CSL 9*R* facet. Moreover, the facet ridges $(100)_{\Sigma3CSL}/9R$ remain sharp up to T_m. The less closely-packed $\Sigma3$ CSL facets appear in Cu with decreasing temperature [34].

In Fig. 2 the EBSD micrograph of the section of Nb bicrystal perpendicular to the common tilt axis $[110]_1/[110]_2$ is shown. The brightness is proportional to the intensity of diffracted [110] peak. Dark line where the primary electron beam meets both grains marks the GB. Six flat portions of GB can be observed. These GB facets are parallel to the CSL planes $(100)_{\Sigma3CSL}$, $\{110\}_{\Sigma3CSL}$, $\{120\}_{\Sigma3CSL}$ and $\{210\}_{\Sigma3CSL}$. It means that the $(100)_{\Sigma3CSL}$ facets are parallel to both $(111)_1$ and $(111)_2$ planes in grains 1 and 2 etc. All these facets

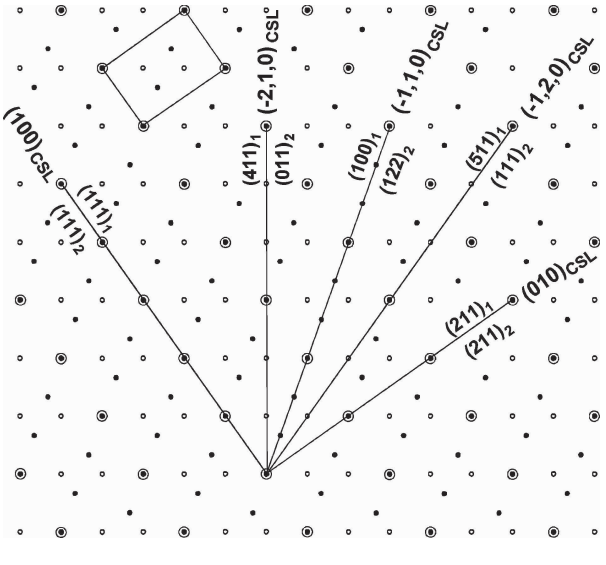

Figure 1 Section of $\Sigma3$ CSL perpendicular to the {110} tilt axis with CSL unit cell and positions of most densely packed CSL planes.

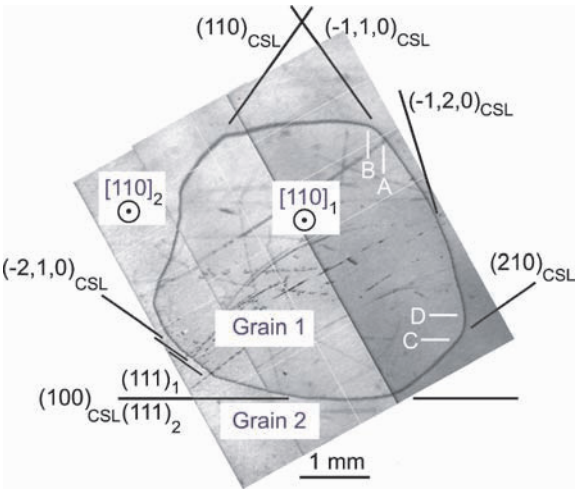

Figure 2 EBSD micrograph of the section of Nb bicrystal perpendicular to the common tilt axis $[110]_1/[110]_2$. The $(100)_{\Sigma 3CSL}$, $\{110\}_{\Sigma 3CSL}$, $\{120\}_{\Sigma 3CSL}$ and $\{210\}_{\Sigma 3CSL}$ facets are marked. The GB curved portions between points *A* and *B*, and *C* and *D* have been digitized in order to determine the critical index β.

do not form the sharp ridges between them. All GB portions between $(100)_{\Sigma 3CSL}$ and $\{210\}_{\Sigma 3CSL}$ facets, between $\{110\}_{\Sigma 3CSL}$ and $\{120\}_{\Sigma 3CSL}$ facets, between $\{210\}_{\Sigma 3CSL}$ and $\{120\}_{\Sigma 3CSL}$ facets are rounded. To the best of our knowledge, curved $\Sigma 3$ twin GBs are observed for the first time. Previously only completely faceted twins were observed in cubic metals like Cu, Ag [34, 35] Ni- and Fe-alloys [19, 36, 37] and polycrystalline Si [38]. Almost all edges between flat GB facets and rounded rough regions are smooth. Similar smooth edges between flat surface facets and rounded rough regions have been observed in lead [26–30] and helium crystals [39]. Near a smooth egde the shape of the curved interface varies as (see Fig. 3)

$$y = A(x - x_0)^{\beta} + \text{higher order terms} \qquad (1)$$

The position of edge is given by x_0. The exponent β is a critical index. Two curved GB regions *AB* between (–1, 2, 0)$_{\Sigma 3CSL}$ and (–1, 1, 0)$_{\Sigma 3CSL}$ facets, and *CD* between (210)$_{\Sigma 3CSL}$ and (–1, 2, 0)$_{\Sigma 3CSL}$ facets have been quantified. The positions of x_0 have been chosen at the edge between flat facet and curved GB portion as in [26] (see scheme in Fig. 3). The respective values were calculated (Fig. 4a and b). $\beta_{AB} = 1.61 \pm 0.09$ for the edge between (–1, 2, 0)$_{\Sigma 3CSL}$ and (–1, 1, 0)$_{\Sigma 3CSL}$ facets. $\beta_{CD} = 1.46 \pm 0.09$ for the edge between (210)$_{\Sigma 3CSL}$ and (–1, 2, 0)$_{\Sigma 3CSL}$ facets. To the best of our knowledge, these are

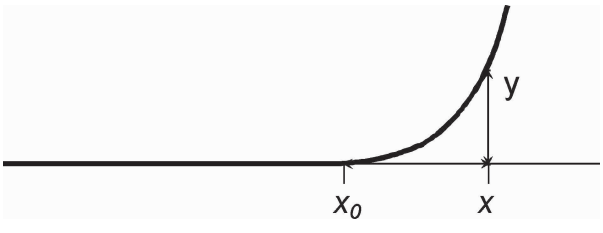

Figure 3 Scheme for the quantification of a curved GB portions *AB* between $(-1, 2, 0)_{\Sigma 3CSL}$ and $(-1, 1, 0)_{\Sigma 3CSL}$ facets, and *CD* between $(210)_{\Sigma 3CSL}$ and $(-1, 2, 0)_{\Sigma 3CSL}$ facets.

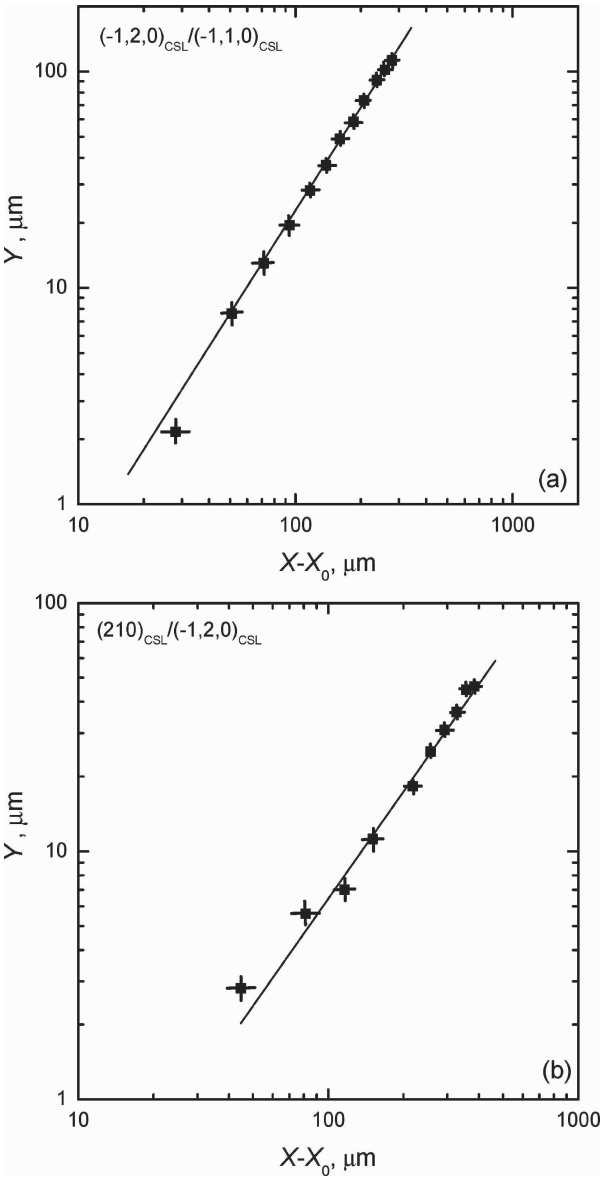

Figure 4 Shape of the rounded GB portions in scaling coordinates. (a) between points *A* and *B* (see Fig. 2) and (b) between points *C* and *D*.

the first critical exponents for GB roughening. There are two main models predicting β values. The mean field approach to the problem of crystal shape neglecting the fluctuations employs a Landau-type expansion of the free energy near the roughening transition of II order [40]. It delivers $\beta = 2$ which is the signature of the square-law effective interaction between steps. The value $\beta = 2$ has never been observed experimentally. Pokrovsky and Talapov discussed the structure of a monolayer deposited on a periodic susbtrate incommensurate with the periodicity of the monolayer itself [41]. The steps occurring in the vicinal surface play the role of the boundaries separating individual commensurate regions in the model [41]. This theory predicts the $\beta = 3/2$. Therefore, we find for the GB roughening the β values which are distinctly below the mean-field prediction and are more consistent with Pokrovsky-Talapov theory. In the recent investigation of ECS of Pb particles it has been observed that critical exponent β measured near a (111) facet is not completely universal and varies with azimutal angle [28]. The β values

distinctly fall into two groups: first mean value is about 1.7 (similar to our value for the edge between (–1, 2, 0)$_{\Sigma 3CSL}$ and (–1, 1, 0)$_{\Sigma 3CSL}$ facets in Nb twin GB) and second is almost equal to 3/2 (similar to our value for the edge between (210)$_{\Sigma 3CSL}$ and (–1, 2, 0)$_{\Sigma 3CSL}$ facets in Nb twin GB). It has been shown that the β value depends on the details of the steps interaction at the vicinal surface. The scanning tunneling microscopy demonstrated that these steps can expose either (100) or (111) microfacets. Higher exponents are connected with (100) step ledges. In our case the difference between measured β for two different facet edges can be due to the similar details of GB steps.

Concerning the free surfaces of crystals it is generally believed that macroscopic equilibrium crystals at temperature $T = 0$ are completely faceted (polyhedral). Theoretical models predict that at nonzero temperatures curved interfacial regions may appear in addition to the planar facets [42]. As T increases, facets shrink and eventually disappear, each facet at its own characteristic roughening (faceting) temperature, T_R until at sufficiently high temperature the equilibrium surface shape becomes everywhere smoothly rounded. In case of $\Sigma 3$ GBs in fcc metals and in Si T_R is higher than T_m, and $\Sigma 3$ GB remains completely faceted up to the melting point. However, in case of Cu $T_R > T_m$ only for two facets (100)$_{\Sigma 3CSL}$ and 9R. For other less closely-packed CSL facets like (100)$_{\Sigma 3CSL}$, T_R is lower than T_m and these facets become stable by decreasing temperature [34]. In case of $\Sigma 3$ GB in Nb both facets and curved GB regions are present close to T_m. Moreover, four crystallographically different CSL facets having different density of coincidence sites are present simultaneously. 9R facet forming the angle of 82° with (100)$_{\Sigma 3CSL}$ facet is absent. Most probably, this facet with its specific structure is stable only in fcc metals like Cu or Ag [34, 35]. From the viewpoint of GB engineering, it means that the $\Sigma 3$ GBs would behave in polycrystalline Nb differently from $\Sigma 3$ GBs in fcc materials. In an fcc material only one $\Sigma 3$ GB inclination [i.e. symmetric twin GB (100)$_{\Sigma 3CSL}$] possesses a very deep energetic minimum [34]. As a result, the equilibrium shape for $\Sigma 3$ GB following from the Wulff construction is a thin elongated twin plate [34]. The elongated twins can be easily recognized in the fcc polycrystal, and the grain shape in such polycrystals with high fraction of $\Sigma 3$ GBs deviates from equiaxial. In Nb several GB inclinations {(100)$_{\Sigma 3CSL}$, {110}$_{\Sigma 3CSL}$, {120}$_{\Sigma 3CSL}$ and {210}$_{\Sigma 3CSL}$} are energetically almost equivalent. It means that even in case of very high fraction of $\Sigma 3$ GBs in Nb polycrystal, the grains would conserve the possibility to remain almost equiaxial.

Authors thank Mr. T. Matsuzaki for the help in OIM measurements. The financial support of Russian Foundation for Basic Research (contracts 04-03-32800 and 04-03-34982), INTAS (grant 03-51-3779) and NATO Linkage grant (PST.CLG.979375) is acknowledged.

References

1. J. M. PAIK, Y. J. PARK, M. S. YOON, J. H. LEE and Y. C. JOO, *Scripta Mater.* **48** (2003) 683.
2. J. S. CHOI and D. Y. YOON, *ISIJ Internat.* **41** (2001) 478.
3. J. B. KOO and D. Y. YOON, *Metal. Mater. Trans. A* **32** (2001) 469.
4. S. B. LEE, D. Y. YOON and M. F. HENRY, *Acta Mater.* **48** (2000) 3071.
5. T. E. HSIEH and R. W. BALLUFFI, *Acta Metall.* **37** (1989) 2133.
6. B. B. STRAUMAL and L. S. SHVINDLERMAN, *ibid.* **33** (1985) 1735.
7. K. HARADA, S. TSUREKAWA, T. WATANABE and G. PALUMBO, *Scripta Mater.* **49** (2003) 367.
8. L. C. LIM and R. RAJ, *Acta Metal.* **32** (1984) 1177.
9. T. WATANABE, Y. SUZUKI, S. TANII and H. OIKAWA, *Philos. Mag. Lett.* **9** (1990) 62.
10. T. WATANABE, K.-I. ARAI, H. TERASHIMA and H. OIKAWA, *Solid State Phenom.* **37–38** (1994) 317.
11. V. RANDLE, *Acta Mater.* **47** (1999) 4187.
12. J. K. MACKENZIE, *Biometrika* **45** (1958) 229.
13. J. B. KOO, D. Y. YOON and M. F. HENRY, *Metal. Mater. Trans. A* **33** (2002) 3803.
14. D. C. CRAWFORD and G. S. WAS, *Met. Trans. A* **23** (1992) 1195.
15. M. SHIMADA, H. KOKAWA, Z. J. WANG, Y. S. SATO and I. KARIBE, *Acta Mater.* **50** (2002) 2331.
16. E. M. LEHOCKEY, G. PALUMBO and P. LIN, *Metal. Mater. Trans. A* **29** (1998) 3069.
17. D. HORTON, C. B. THOMPSON and V. RANDLE, *Mater. Sci. Eng. A* **203** (1995) 408.
18. M. KUMAR, A. J. SCHWARZ and W. E. KING, *Acta Mater.* **50** (2002) 2599.
19. T. SCHOBER and D. H. WARRINGTON, *Phys. Stat. Sol.* (a) **6** (1971) 103.
20. G. DHALENNE, M. DECHAMPS and A. REVCOLEVSCHI, *J. Am. Ceram.* **65** (1982) C11.
21. D. J. DINGLEY and R. C. POND, *Acta Metall.* **27** (1979) 667.
22. G. HASSON and C. GOUX, *Scripta Metall.* **5** (1971) 889.
23. J. W. MATTHEWS, *ibid.* **11** (1977) 233.
24. A. OTSUKI and M. MITSUNO, *Trans. Jap. Inst. Met. Suppl.* **27** (1986) 789.
25. T. SCHOBER and R. W. BALLUFFI, *Phil. Mag. A* **21** (1970) 109.
26. C. ROTTMAN, M. WORTIS, J. C. HEYRAUD and J. J. MÉTOIS, *Phys. Rev. Lett.* **52** (1984) 1009.
27. S. SURNEV, K. ARENHOLD, P. COENEN, B. VOIGTLANDER, H. P. BONZEL and P. WYNBLATT, *J. Vac. Sci. Technol. A* **16** (1998) 1059.
28. K. ARENHOLD, S. SURNEV, P. COENEN, H. P. BONZEL and P. WYNBLATT, *Surf. Sci.* **417** (1998) L1160.
29. K. ARENHOLD, S. SURNEV, H. P. BONZEL and P. WYNBLATT, *ibid.* **424** (1999) 271.
30. H. P. BONZEL and A. EMUNDTS, *Phys. Rev. Lett.* **84** (2000) 5804.
31. V. G. GLEBOVSKY, V. V. LOMEYKO and V. N. SEMENOV, *J. Less-Common Metals* **117** (1986) 385.
32. V. N. SEMENOV, B. B. STRAUMAL, V. G. GLEBOVSKY and W. GUST, *J. Crystal Growth* **151** (1995) 180.
33. U. WOLF, F. ERNST, T. MUSCHIK, M. W. FINNIS and H. F. FISCHMEISTER, *Phil. Mag. A* **66** (1992) 991.
34. B. B. STRAUMAL, S. A. POLYAKOV, E. BISCHOFF, W. GUST and E. J. MITTEMEIJER, *Interface Sci.* **9** (2001) 287.
35. A. BARG, E. RABKIN and W. GUST, *Acta Metall. Mater.* **43** (1995) 4067.
36. S. B. LEE, D. Y. YOON and M. F. HENRY, *Metall. Mater. Trans. A* **34** (2003) 1433.
37. G. D. SUKHOMLIN and A. V. ANDREEVA, *Phys. Stat. Sol.* (a), **78** (1983) 333.
38. Z.-J. WANG, S. TSUREKAWA, K. IKEDA, T. SEKIGUCHI and T. WATANABE, *Interface Sci.* **7** (1999) 197.
39. Y. CARMI, S. G. LIPSON and E. POLTURAK, *Phys. Rev. B* **36** (1987) 1894.
40. A. F. ANDREEV, *Sov. Phys. JETP* **53** (1981) 1063.
41. V. L. POKROVSKY and A. L. TALAPOV, *Phys. Rev. Lett.* **42** (1979) 65.
42. C. ROTTMAN and M. WORTIS, *Phys. Rep.* **103** (1984) 59.